Gloss optical elementary representative surface

Pierre Vernhes,* Jean-Francis Bloch, Anne Blayo, and Bernard Pineaux

Ecole Française de Papeterie et des Industries Graphiques (EFPG),
461 rue de la papeterie, BP 65, 38402 Saint-Martin d'Hères, France

*Corresponding author: pierre.vernhes@efpg.inpg.fr

Roughness measurements are of main importance in characterizing the optical properties of papers and prints. However, there is a lack of knowledge concerning the surface size and the spacing of the measures to be optically representative of the surface structure. Paper is a multiscale medium, and the roughness parameters extracted from the three-dimensional (3D) surface mapping depend on both the size and the step of discretization. Ray tracing, based on optical geometry, could be a tool to model the light reflection on a paper surface. Ray-tracer software was therefore developed. A new optical device was used to measure paper surface topographies at various scales. Ray tracing simulations were then performed on the 3D mapping and compared to the scattering indicatrix obtained with a classical goniometer. Hence it was possible to identify a magnification for various types of paper grades that is optically representative of the specular gloss. © 2008 Optical Society of America

OCIS codes: 080.0080, 080.1753, 240.5770, 240.6700.

1. Introduction

Paper is a complex composite material. Its structure and its surface greatly influence its runnability and its printability [1,2]. The paper surface characterization is crucial for understanding light reflection and scattering that control the level of gloss [3–10]. The paper surface topography can be described with different techniques, such as air leakage instruments, stylus technique, or optical devices [11–14] including scanning electron microscopy (SEM), atomic force microscopy (AFM), confocal laser scanning microscopy (CLSM), laser profilometer, interferometry, and chromatic aberration. New optical devices based on the focus variation technique allow a mapping of the paper surface with a submicron precision [15] at various scales. Paper is a multiscale medium, and the roughness parameters extracted from the three-dimensional (3D) mapping depend on both the sample size and the spacing used during the measurement. The aim of this paper is to relate the specular gloss of paper to a representative size of surface measured and to predict the paper gloss from topo-

graphical data. Using a focus variation device (IFM from Alicona), the paper surface properties of five paper samples at different magnifications (×5, ×10, ×20, ×50, and ×100) were studied. Thus paper topography was characterized with surface sizes varying from $80 \, \mu m \times 80 \, \mu m$ with a spacing of $80 \, nm$ to a size of $1.6 \, mm \times 1.6 \, mm$ with a spacing of $1.6 \, \mu m$. The technology on which the system is based has recently been included into International Organization for Standardization (ISO) standards [16] classifying different methods for surface texture extraction.

The reflected light is an electromagnetic radiation operating in the visible spectrum, which interacts with the surface of an object. The incident light may be composed of several rays of different distributed wavelengths. In the case of visible light the electromagnetic radiation includes wavelengths between $380 \, nm$ and $780 \, nm$. The interaction between light and the media can be separated into the reflection by the bulk and the reflection by the surface. The bulk scattering is an interaction within the thickness of the material that leads to diffused light [17–19]. The specular reflection is a surface interaction, reflecting light in an angle symmetric to the angle of incidence (in the case of a smooth surface) in respect

to the normal of the considered surface. Gloss is defined by the American Society of Testing and Materials (ASTM) as "the angular selectivity of reflectance involving surface reflected light, responsible for the degree to which reflected highlights or images of objects may be seen as superimposed" [20]. For paper and print media, the bulk scattering is essential because it is responsible for the color appearance, as the incident spectrum may be modified by absorption of some radiations. The specular reflection preserves the spectrum of the incident light. Nevertheless, paper gloss is often associated with high quality and therefore efforts are made to fulfill customer demands [21]. Concerning the prints, the level of gloss required depends on the application. It can be seen as a distortion that may hide the information intended to be conveyed by the print [22]. The visual perception of gloss has been the object of numerous studies [6,23,24]. For example, Hunter [25] identified six different criteria related to the visual perception of gloss; specular gloss, sheen, contrast gloss or luster, absence of bloom gloss, distinctness of image gloss, and the surface uniformity of gloss.

The factors affecting the gloss and the gloss uniformity of an object are numerous. The illumination conditions (light source and light intensity) are of main importance as well as the detection conditions (detector type and geometry of the system). The sample parameters (surface roughness and refractive index) are obviously crucial [5]. The two main surface descriptors used in the literature are commonly the root mean square (rms or S_q in the case of a two-dimensional (2D) surface) and the lateral correlation (or correlation length denoted L_c). The surface topography, especially the angle between the normal of the local microfacet and the incident direction, plays a major role in the perception or measurement of gloss [26]. The multiple scattering of light on the surface has also to be taken into account to accurately predict the gloss from topographical measurement [26].

The scattering of electromagnetic waves on rough surfaces is of main importance in various fields such as optics astronomy and cosmetics. Nevertheless, analytical solutions are limited to certain conditions. In most of the models, height distribution is assumed to follow a Gaussian curve [27]. However, this is not the case for paper and print samples. Fractal distribution may also be used [28]. Furthermore, most of these models applied for a one-dimensional (1D) profile. The main theories of light scattering on a rough surface are based on the Kirchhoff approximation, the integral method, the small perturbation method, the small slope approximation, and the phase perturbation theory [29]. A review of these models was recently published by Hermansson [30]. The gloss level is analytically associated with the "rms" of the surface considered and either the correlation length or the power spectrum of the surface roughness. Nevertheless, these models are unable to predict either the

shadowing or masking effect or the multiple scattering, which can be extensive for large incident angles and rough surfaces [13]. Another crucial point is that paper is composed of different roughness scales [31]. Hence the values of S_q and L_c may vary as a function of the step of discretization and the surface size of the sample.

Optical geometry through ray tracing could be a tool to model light reflection on a paper surface. The numerical technique of ray tracing is implemented by launching a large number of rays onto the surface, and each ray is traced through its reflections on the surface until it escapes [30]; Fresnel reflection is applied to each local point of contact. The geometric optics approximation to electromagnetic theory was computed with Matlab. We assume that in case of paper and paper coatings, the criteria based on the correlation length, the rms, and the wavelength are fulfilled [32,33]. Therefore the facet model is acceptable [34–36].

The main parameters of this virtual goniometer can be modified, such as the goniometer geometry, the intensity of the light, and the spatial positions of both the receptor and the lamp. Then, ray tracing simulations were performed on the three-dimensional (3D) mapping and compared to the scattering indicatrix obtained with a standard goniometer. Hence it was possible to identify a magnification for various types of paper grades, which is optically representative of the specular gloss assuming the Fresnel reflectance approximation.

2. Material and Method

A. Description of the Topographic Equipment

We used the infinite focus measurement machine (IFM), which is an optical measurement device that allows for the acquisition of datasets at high depth of focus, similar to the SEM.

The main component of this optical metrology instrument is a precision optic consisting of various lens systems. It can be equipped with different objectives allowing measurements with different resolutions. With a beam splitting mirror, light emerging from a white light source is inserted into the optical path of the system and focused onto the specimen via the objective. Depending on the topography of the specimen, the light is reflected into several directions as soon as it hits the specimen. All rays emerging from the specimen and hitting the objective are bundled in the optics and gathered by a light sensitive sensor behind the beam splitting mirror.

Due to the small depth of field of the optics, only small regions of the object are sharply imaged. To allow a complete detection of the surface with full depth of field, the precision optic is moved vertically along the optical axis. A sensor captures a series of 2D datasets during this scanning process. All sensor parameters are optimized at each vertical position according to the reflective properties of the surface. After the scanning process, the 2D datasets are

evaluated to generate 3D information. This is achieved by analyzing the variation of focus along the vertical axis. Once all height measurements are determined, an image with full depth of field is computed. In this technique, the surface topography is measured independently of surface reflectivity as long as the local brightness lies between the black and white levels that the camera can handle. The topography is measured from the calculation of the maximum focusing distance. At the maximum focusing, the distance between the surface and the objective is always the same for a given objective. Consequently, every point measured at the maximum focusing has been acquired using the same collection angle.

A key characteristic of the system is that it not only delivers topographical information but also an optical color image of the surface. The technology on which the system is based has recently been included into ISO standards [16] classifying different methods for surface texture extraction. Five different objectives were used: ×5, ×10, ×20, ×50, and ×100, giving a lateral resolution of $1.6\,\mu m$, $800\,nm$, $400\,nm$, $160\,nm$, and $80\,nm$, respectively. For the ×100 and ×50 magnifications, the sampling distance is shorter than the light wavelength. Hence the lateral resolution is limited by the light wavelength and specified to be $400\,nm$. However, the apparent resolution is $160\,nm$ and $80\,nm$, respectively. The image resolution is 1024×1280 pixels, coded into 16 bits. A typical measurement takes about one minute.

Parameters are calculated according to the mean plan. No data treatment is carried out; only the raw data are treated in order to compare the different scales of measurements. Samples were put on a stage to ensure a good flatness.

The suitability of the paper roughness measurement using the IFM has been recently demonstrated [37] by comparing the surface roughness obtained using different devices (such as the air leakage method and optical and mechanical profilometry).

B. Goniometer

The scattering indicatrix was measured using an ETA-Optik (now AudioDev GmbH) spectrophotogoniometer. The angle of the incident light was 75° to fit the requirements of the Technical Association of the Pulp and Paper Industry (TAPPI) standard as generally accepted for paper gloss measurement. The working distance is $100\,mm$, the diameter of the optical aperture is $2\,mm$, and the size of the measuring spot is $0.7\,mm$. The source is a $50\,W$ halogen light with a color temperature of $3000\,K$. We chose the wavelength of $550\,nm$ for the measurements.

C. Physical Paper Properties

We chose two commonly used office papers referenced as Q+ and Q−, respectively. These papers are common office papers: Q+ is assumed to have a better quality than Q−. We also studied two inkjet papers, one of high quality (used for photographic

purposes) referenced as Jet+ and another referenced as Jet−. Finally a coated paper was also analyzed (referenced as C).

Paper properties (basis weight, thickness and Beck roughness, PPS and Bendtsen) were measured (Table 1).

3. Theory

A. Gloss

Gloss is related to the capability of a surface to reflect light directly [25]. The term gloss includes a large variety of surface phenomena constituting the light-reflecting properties of a surface. The most well known type of gloss, and the one we will focus on, is the specular gloss. Specular reflectance is defined as the ratio of the intensity of the reflected beam to the intensity of the incident beam at a specific angle of incidence. The angle of incidence, θ, is referenced to the surface normal.

For isotropic, homogeneous, optically smooth surfaces that do not present diffuse reflection and are essentially nonabsorbing, specular reflectance is only governed by the index of refraction, the angle of incidence of the light, and the polarization state of the incident light. For optically smooth surfaces (such as a mirror), the specular reflectance can be calculated from Fresnel's theory [38]:

$$\rho(\theta,\lambda) = \frac{1}{2} * \left[\left(\frac{\cos\theta - \sqrt{n(\lambda)^2 - \sin^2(\theta)}}{\cos\theta + \sqrt{n(\lambda)^2 - \sin^2(\theta)}} \right)^2 + \left(\frac{n(\lambda)^2 \cos\theta - \sqrt{n(\lambda)^2 - \sin^2(\theta)}}{n(\lambda)^2 \cos\theta + \sqrt{n(\lambda)^2 - \sin^2(\theta)}} \right)^2 \right], \quad (1)$$

where $n(\lambda)$ is the index of refraction at the wavelength λ.

In the case of the paper surface, the rough and anisotropic nature of the surface brings tremendous difficulties to model the specular reflectance of the paper surface.

Chinmayanadam proposed a modeling relating the gloss of a surface to its roughness. He assumed that the elements responsible for the gloss were normally distributed. Hence he suggested the expression given in Eq. (2) for the scattered intensity I:

$$I = \exp\left(-\frac{8\pi^2 \cos^2 R}{\alpha\lambda^2} \right), \quad (2)$$

Table 1. Physical Paper Properties

	Q−	Q+	C	Jet−	Jet+
Basis-Weight (g/m^2)	81.2	120.4	114.7	126.8	255.6
Thickness (μm)	110.8	124.7	92.0	163.6	273.0
PPS (μm)	5.8	3.2	1.8	3.4	Out of Range
Bendtsen (mL/min)	129.6	25.0	13.9	38.9	OOR
Bekk (s)	16.9	109.2	517.1	93.8	>20000

where R is the view angle, α a constant in m^{-2}, and λ the wavelength.

Improvements of Eq. (2) were made to take into account specifically the surface roughness [23,39]:

$$\frac{I}{I_0} = \rho(\theta, \lambda) \exp\left(\left(-\frac{4\pi\sigma \times \cos\theta}{\lambda}\right)^2\right), \qquad (3)$$

where the roughness σ is equal to (S_q) for Gaussian distribution, ρ is the Fresnel reflectance, and I_o is the intensity of the incoming beam light.

Equation (3) has been intensively used. However, many cases of surfaces with close values of S_q but with different values of gloss were reported [40].

Besides, one of the assumptions adopted in Eq. (3) is that the surface roughness is smaller than the wavelength. In the visible range, such a condition is achieved for only a few types of paper grades (coated papers or photographic papers, for instance). Other interesting attempts have been made to apply modified scattering models on paper surface or surface comparable to paper [31,35,36,38,41,42].

B. Statistical Parameters

S_q is a dispersion parameter defined as the rms value of the surface departures, z, from the local plane within the sampling area:

$$S_q = \sqrt{\frac{1}{MN}\sum_{j=1}^{N}\sum_{i=1}^{M} z^2(x_i, x_j)}, \qquad (4)$$

where M is a number of points of each profile, and N is the number of profiles.

To characterize the lateral feature of the surface, the correlation length was chosen.

The first parameter is the areal autocovariance function (ACVF) defined as

$$\mathrm{ACVF}(\tau_x, \tau_y) = \frac{1}{(L_x - \tau_x)(L_y - \tau_y)}$$
$$\int_0^{(L_x - \tau_x)}\int_0^{(L_y - \tau_y)} z(x,y)z(x + \tau_x, y + \tau_y)\mathrm{d}x\mathrm{d}y, \quad (5)$$

where τ_x and τ_y are the lags in the x and y directions, L_x and L_y are the profile lengths in the x and y directions, and $z(x,y)$ is the height at the x, y position on the surface.

By normalizing the ACVF, the areal autocorrelation function (AACF) is obtained:

$$\mathrm{AACF} = \frac{\mathrm{ACVF}(\tau_x, \tau_y)}{\mathrm{ACVF}(0,0)}. \qquad (6)$$

The correlation length (L_c) is the value for which the AACF is decreased to a factor $(1/e)$ of its value at zero lag.

As paper surface topography can be anisotropic, the correlation length is directionally dependent.

C. Ray Tracing

Optical geometry through ray tracing is a useful tool to model the light reflection on a paper surface. The numerical technique of ray tracing is implemented by launching a large number of rays on the surface. Each ray is traced through its reflections on the surface until it escapes [30]; Fresnel reflection is applied to each local point of intersection. For rough surfaces, the number of contacts of a ray before leaving the surface typically increases with increasing surface slopes. Specular (Fresnel) and diffuse (Lambertian) models are often used in geometric optics. In the specular model, energy is reflected in the solid angle region around the specular angle, and the fraction of the energy that is reflected is found using the Fresnel equations. In the diffuse model, the energy is equally distributed in all directions [43].

Tang [32,33,44] studied the accuracy of the approximation function of the normalized correlation τ/λ and the normalized surface roughness σ/λ for 2D surfaces. He stated that if the two normalized surface descriptors (τ/λ and σ/λ) are greater than unity (which is the case for most common paper), optical geometry leads to accurate results. Furthermore, in some special cases, the approximation can yield to an accurate solution even if both parameters are less than unity. This technique permits a complete description of the shadowing effect occurring for large angles of incidence. Furthermore, the multiple scattering on the surface could be easily calculated. Figure 1 presents a schematic representation of a multiple surface scattering.

4. Results and Discussion

A. Influence of the Magnification on the Surface Parameters

Figure 2 demonstrates the relation between the S_q value of the paper grade considered and the magnification chosen for the measurement for the objectives ×5 ×10 ×20 ×50 and ×100. The presented results are averaged for 20 measurements.

The S_q values of the samples considered decrease with the increasing magnification. In fact, reducing the field of measurement (while keeping the same number of points taken into account) acts as a filter. Only the smallest roughness wavelengths
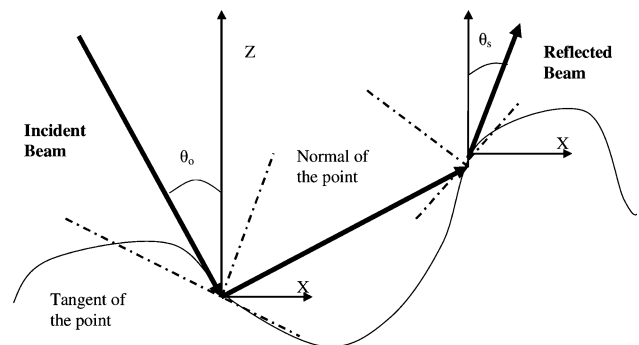

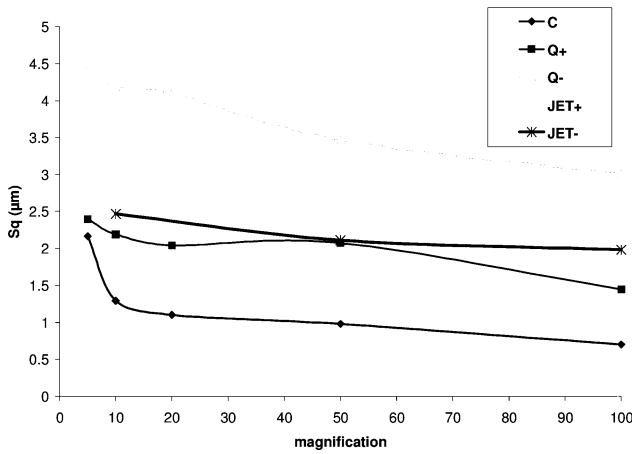Fig. 1. Rough surface scattering geometry [44].

Fig. 2. S_q variation versus magnification on five paper samples.

are maintained with the bigger objectives. The S_q evolution of the JET+ sample is remarkable. S_q value can be divided by a factor of 6 from 292 nm (×20) down to 44 nm (×100). This result is fundamental in understanding the influence of the surface size and of the step of discretization of the measurement, in the interpretation of surface roughness results. The influence of these two factors, sample size and step of discretization, has been recently studied [37]. Indeed, measurements on large areas take into account undulation due to large roughness wavelengths created for example during the sheet formation. But on the other hand, large magnifications (small area measurements with high discretization) characterize the microroughness.

B. Three-Dimensional Numerical Goniometer

The geometric optics approximation to electromagnetic theory was computed using Matlab. The number of intersections between the rays and the surface depends on the roughness parameters and especially on the surface slopes. Typically, the number of intersections increases with the mean slope. For a totally flat surface, the problem is reduced to the Fresnel equation since all the energy is reflected in the solid angle around the specular angle [32]. A virtual lamp was hence constructed. It consists of a disk with equally distributed points in the plan direction. The spacing between the points depends on the energy to be sent, that is, the number of rays sent on the surface to be tested. The position of the virtual lamp regarding the sample can be adjusted around the hemisphere above the sample plane by regulating the polar angle θ and the azimuthal angle ϕ. From all the nodes of the lamp emerge rays that are sent onto the surface. The direction of incidence of the rays is expressed as follows:

$$\vec{V}_o = x\vec{i} + y\vec{j} + z\vec{k}, \tag{7}$$

where

$$x = \sin(\phi_0)\cos(\theta_0), \tag{8}$$

$$y = \sin(\phi_0)\sin(\theta_0), \tag{9}$$

$$z = \cos(\theta_0). \tag{10}$$

The first reflection points are determined by calculating the intersection of the distributed vectors emerging from the lamp and the surface. This intersection point may not be necessarily a node of the surface mapping. In fact, the intersection is calculated by solving the two equations of the projection of the vectors and the surface in both the xOy and xOz planes. From the intersection point, the normal of the local facet is calculated. The direction of the reflected ray $\vec{V}_s$ is found by using Snell's first law, which states that the angle between the incident and normal vector, $\vec{n}$, is equal to the angle between the reflected and normal vector. According to the angle between the incident ray and the normal of the facet, the energy carried by the reflected ray is determined by the Fresnel coefficient. The same procedure is applied to the reflected ray at each reflection until it leaves the surface.

There are two implemented ways to analyze the reflected rays. A virtual receptor can collect the rays. The geometry and the spatial position of this receptor can be adjusted to fit the geometry of real goniometer, to test the influence of the geometry on gloss results. Another definition of gloss is the fraction of the light that is scattered into a small angular interval $\Delta\theta$ around the specular direction. The specular direction is noted Θ, and according to the previous definition the acceptable direction to be considered glossy is $\theta_\pm = \Theta \pm \Delta\theta$. This last definition permits one to plot the histogram of the angles of the reflected rays.

C. Comparison between the Experimental Data and the Simulated Results

Twenty topographic measurements were carried out for each paper grade at each magnification. The following setup was then fixed for each ray tracing simulation. 50000 rays were sent onto each measured surface. Indeed, from the discrete numerical values, the surface is reconstructed using linear interpolation for the calculation of the slopes. The distance of the lamp from the center of the sample was 1000 μm. The radius of both the lamp and the receptor was 250, 120, 60, 25, and 12 μm, corresponding to ×5, ×10, ×20, ×50 and ×100, respectively.

Table 2 presents values of the maximum of the scattering indicatrix obtained with the goniometer for the five papers considered and the simulated results according to the magnification used (the values were normalized to JET+). The coefficient R^2 is the correlation coefficient between the experimental and simulated values for a linear regression $y = x$.

Table 2 demonstrates that the ray tracing method is suitable to predict the paper gloss. As a matter of fact, the correlation coefficient between the

Table 2. Value of the Maximum Scattering Indicatrix for Experimental and Simulated Results for Five Paper Samples

|	Goniometer Measurements	×5	×10	×20	×50	×100
Q–	**0.02**	0.36	0.18	0.09	0.04	0.02
Q+	**0.05**	0.43	0.35	0.19	0.05	0.04
C	**0.26**	0.42	0.55	0.42	0.33	0.24
JET+	**1.00**	1.00	1.00	1.00	1.00	1.00
JET–	**0.02**	0.25	0.17	0.09	0.04	0.02
R^2 Numerical/ Measurement		**0.35**	**0.51**	**0.91**	**0.98**	**0.99**

Fig. 3. Comparison between experimental and simulated scattering indicatrix for three papers (×100 magnification).

experimental and simulated gloss values for the ×50 and ×100 magnifications is close to unity.

Furthermore, to relate the topographic information to the optical measurement, the constituent lateral size of the sample is crucial. For instance, the ×5 magnification does not allow a ranking of the gloss level of the papers considered, since, for example, Q+ simulated gloss level is above C. For magnification above ×10, the ranking is respected, and the correlation coefficient is getting close to 1 with an increase in the magnification. The best simulated gloss levels are obtained for the highest magnifications, ×50 and ×100. The main axis of the virtual light spot on the measured surface is about $100\,\mu m$ and $50\,\mu m$, respectively. On the other hand, the size of the real spot of the goniometer on the paper surface is about 3 mm, which is 50 times bigger. In fact, the results are the average of 20 simulations on 20 topographical measurements. Hence even if the sizes of the simulation are small and may be better related to microgloss [5,7–9,21] than macrogloss, the overall mean is closely related to the macroscopic measurements.

Gloss homogeneity on a paper surface is of main importance, as a distortion can arise from surface heterogeneity and can cause print mottle. Table 3 exhibits the value of the dispersion of the gloss value for the magnifications ×50 and ×100. The dispersion is defined as the ratio between the standard deviation and the mean.

Interesting conclusions can be drawn from Table 3. The dispersions get smaller when the magnifications increase, except for paper Q–. The virtual gloss dispersion is closely related to the paper quality since the two worst dispersions were obtained for Q– and JET–, and the best correspond to JET+.

Figure 3 exhibits the simulated indicatrices obtained from the ×100 measurements. To facilitate reading, only the paper JET+, C, and Q– are shown.

The widths of the simulated curves are wider than the measured one. In fact, due to the small size of the sample measured, it was not possible to adjust both
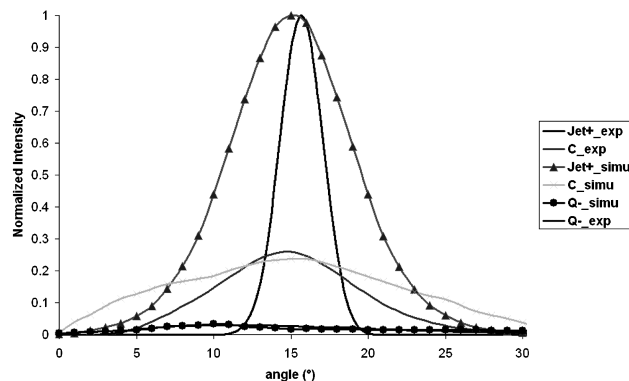
the distance and the radius of the lamp (and receptor) to obtain the experimental goniometric solid angle of illumination. This behavior is amplified for large magnifications.

5. Conclusion

This paper aims at calculating the representative illuminated surface and roughness measurement size of paper regarding the specular gloss. A focus variation device permits the study of the paper surface topography at various scales. The magnification allows for the analysis of different correlated sizes of paper surface. Hence the evolution of the two main surface parameters (S_q and L_c) was studied as a function of the magnification. The evolution of these parameters strongly depends on the paper grade. Nevertheless, S_q and L_c decrease nonlinearly with the augmentation of the magnification. These preliminary results underline the difficulties for specular scattering analytical resolution of multiscale media such as paper and print. That is why the geometric optics approximation to electromagnetic theory was computed with Matlab. A virtual goniometer was hence built up. The main parameters of the virtual goniometer can be regulated, such as the goniometer geometry, the intensity of the light, and the special positions of both the receptor and the lamp. Then ray tracing simulations were performed on the 3D mapping and compared to the scattering indicatrix obtained with a standard goniometer. Hence it was possible to isolate a magnification for various types of paper grades, which is optically representative of the specular gloss. The best fits between the simulated and experimental scattering indicatrices were obtained for the surface measured with large magnification. Furthermore, by analyzing the dispersion of the virtual gloss, it is possible to assess the optical uniformity of the paper surface.

Table 3. Gloss Dispersion of the Simulated Results

	Q–	Q+	C	JET–	JET+
×50	0.20	0.54	0.15	0.08	0.14
×100	0.15	0.61	0.11	0.03	0.13

References

1. J. F. Bloch, S. Rolland du Roscoat, C. Mercier, P. Vernhes, B. Pineaux, A. Blayo, and P. Mangin, "Influence of paper structure on printability: characterization using x-ray synchrotron microtomography," in *NIP22: International Conference on Digital Printing Technologies* (Society for Imaging Science and Technology, 2006), pp. 449–453.

2. P. Vernhes, C.-S. Rolland du Roscoat, A. Blayo, B. Pineaux, and J. F. Bloch, "Synchrotron x-ray microtomography: a new tool to characterize the interaction between paper and toner," J. Imaging Sci. Technol. **52**, 6 (2008).

3. G. Chinga, "Detailed characterization of paper surface structure for gloss assessment," J. Pulp Pap. Sci. **30**, 222–227 (2004).

4. G. Chinga and T. Helle, "Relationships between the coating surface structural variation and print quality," J. Pulp Pap. Sci. **29**, 179–184 (2003).

5. M. C. Beland, S. Lindberg, and P. A. Johansson, "Optical measurement and perception of gloss quality of printed matte-coated paper," J. Pulp Pap. Sci. **26**, 120–123 (2000).

6. M. C. Beland and L. Mattsson, "Optical print quality of coated papers," J. Pulp Pap. Sci. **23**, 493–498 (1997).

7. J. S. Arney, L. Ye, J. Wible, and T. Oswald, "Analysis of paper gloss," J. Pulp Pap. Sci. **32**, 19–23 (2006).

8. J. S. Arney, H. Heo, and R. G. Anderson, "A microgoniophotometer and the measurement of print gloss," J. Imaging Sci. Technol. **48**, 458–463 (2004).

9. J. S. Arney, J. Michel, and K. Pollmeier, "Technique for analysis of surface topography of photographic prints by spatial analysis of first surface reflectance," J. Imaging Sci. Technol. **46**, 350–358 (2002).

10. T. Pettersson and A. Fogden, "Leveling during toner fusing: effects on surface roughness and gloss of printed paper," J. Imaging Sci. Technol. **50**, 202–215 (2006).

11. G. Chinga, T. Stoen, and O. W. Gregersen, "On the roughening effect of laboratory heatset offset printing on SC and LWC paper surfaces," J. Pulp Pap. Sci. **30**, 307–311 (2004).

12. P. Aslund, P. A. Johansson, and E. Blohm, "Photometric method for dynamic measurements of paper roughening after a moistening printing nip," Nord. Pulp Paper Res. J. **19**, 460–465 (2004).

13. I. Arino, U. Kleist, G. G. Barros, P. A. Johansson, and M. Rigdahl, "Surface texture characterization of injection-molded pigmented plastics," Polym. Eng. Sci. **44**, 1615–1626 (2004).

14. J. S. Aspler and M. C. Beland, "A review of fiber rising and surface roughening effects in paper," J. Pulp Pap. Sci. **20**, 27–32 (1994).

15. S. Hartmuth, S. Mario, and S. Stefan, "Comparison of 3D surface reconstruction data from certified depth standards obtained by SEM and an infinite focus measurement machine (IFM)," Microchim. Acta **155**, 279–284 (2006).

16. ISO 25178-6, "Geometrical product specifications (GPS)—surface texture: areal. Part 6. Classification of methods for measuring surface texture," (ISO, 2008).

17. H. Granberg and M. C. Beland, "Modelling the angle-dependent light scattering from sheets of pulp fibre fragments," Nord. Pulp Paper Res. J. **19**, 354–359 (2004).

18. M. Lindstrand, "Gloss: measurement, characterization and visualization in the light of visual evaluation," Ph.D. dissertation (Linkopings Universitet, 2002).

19. P. Edstrom, "Mathematical modelling of light scattering in paper and print," Ph.D. dissertation (Mid Sweden University, 2004).

20. "Standard terminology of apparence," A. E284 (American Society of Testing and Materials, 1999).

21. M. C. Beland and J. Bennet, "Effect of local microroughness on the gloss uniformity of printed paper surfaces," Appl. Opt. **39**, 2719–2726 (2000).

22. R. M. Leekley, C. W. Denzer, and R. F. Tyler, "Measurement of surface reflection from papers and prints," Tappi J. **53**, 615–621 (1970).

23. D. I. Lee, "A fundamental study on gloss," in *TAPPI 1974 Coating Conference Proceedings* (TAPPI, 1974), pp. 97–103.

24. M. Lindstrand, "Gloss characterization by angularly and spacially resolved reflectometry in the light of visual evaluation," J. Imaging Sci. Technol. **49**, 61–70 (2002).

25. R. Hunter, ed., *The Measurement of Appearance* (Wiley, 1987).

26. M. C. Beland, "Multiple scattering of light calculated from the topography of printed paper surfaces," Appl. Opt. **39**, 2719–2726 (2000).

27. R. Alexandra-Katz and R. G. Barrera, "Surface correlation effect on gloss," J. Polym. Sci. Part B Polym. Phys. **36**, 1321–1334 (1998).

28. G. Lixin and W. Zhensen, "Application of FFT to light scattering from one-dimensional fractal rough surface," Microw. Opt. Technol. Lett. **35**, 317–322 (2002).

29. I. Simonsen, A. Larsen, E. Andreassen, E. Ommundsen, and K. Nord-Varhaug, "Estimation of gloss from rough surface parameters," Phys. Status Solidi A **242**, 2995–3000 (2005).

30. P. Hermansson, G. Forssell, and J. Fagerstrom, "A review of models for scattering from rough surfaces" (Swedish Defense Research Agency, 2003).

31. N. J. Elton, "A two-scale roughness model for the gloss of coated paper," J. Opt. A **10**, 085002 (2008).

32. K. Tang and R. O. Buckius, "A statistical model of wave scattering from random rough surfaces," Int. J. Heat Mass Transfer **44**, 4059–4073 (2001).

33. K. Tang, R. Dimenna, and R. Buckius, "Region of validity of the geometrics optics approximation for angular scattering from very rough surface," Int. J. Heat Mass Transfer **40**, 49–59 (1996).

34. V. G. W. Harrison, "Gloss measurement of papers: application of the Barkas analysis," Br. J. Appl. Phys **1**, 46–53 (1950).

35. L. F. Gate and D. J. Parsons, "The specular reflection of polarized light from coated paper," in *Transactions of the 10th Fundamental Research Symposium* (Oxford University, 1993), pp. 263–284.

36. T. R. Lettieri, E. Marx, J. Song, and T. V. Vorburger, "Light scattering from glossy coatings on paper," Appl. Opt. **30**, 4439–4447 (1993).

37. P. Vernhes, J. F. Bloch, A. Blayo, C. Mercier, and B. Pineaux, "Statistical analysis of paper surface microstructure: a multi scale approach," Appl. Surf. Sci. **254**, 7431 (2008).

38. I. Arino, U. Kleist, L. Mattsson, and M. Rigdahl, "On the relation between surface texture and gloss of injection-molded pigmented plastics," Polym. Eng. Sci. **45**, 1343–1356 (2005).

39. P. S. Beckmann and A. Spizzochino, *The Scattering of Electromagnetic Waves from Rough Surfaces* (Pergamon Press, 1963).

40. V. Bliznyuk, H. Assender, and K. Porfyrakis, "How surface topography relates to material's properties," Mater. Sci. Eng. B **297**, 973–976 (2002).

41. L. Gate, W. Windle, and M. Hine, "The relationship between gloss and surface microstructure of coatings," Tappi J. **56**, 61–65 (1973).

42. M. A. Macgregor and P. Johansson, "Submillimetre gloss variations in coated paper. Part 1: The gloss imaging equipment and analytical techniques," Tappi J. **73**, 161–168 (1990).

43. K. E. Torrance, "Monochromatic directional distribution of reflected thermal radiation from roughened dielectric surfaces," Ph.D. dissertation (University of Minnesota, 1964).

44. K. Tang and R. Buckius, "The geometrics optics approximation for reflection from two dimensional random rough surfaces," Int. J. Heat Mass Transfer **41**, 2037–2047 (1998).